A High Step -Up Solar Power Optimizer with Switched Capacitor and Coupled Inductor Technology with MPPT Technique

J. Praveena
Student, Department of EEE, Kuppam Engineering College, Kuppam, Andhra Pradesh, India
Y. Dhamodharam
Associate Professor, Department of EEE, Kuppam Engineering College, Kuppam, Andhra Pradesh, India
N. Venugopal
Professor, HOD, Department of EEE, Kuppam Engineering College, Kuppam, Andhra Pradesh, India

Abstract:
This paper proposes a high step-up solar power optimizer (SPO) that efficiently harvests maximum energy from a photovoltaic (PV) panel then outputs energy to a dc-microgrid. Its structure integrates coupled inductor and switched capacitor technologies to realize high step-up voltage gain. The leakage inductance energy of the coupled inductor can be recycled to reduce voltage stress and power losses. A low voltage rating and low-conduction resistance switch improves system efficiency by employing the incremental conductance method for the maximum power point tracking (MPPT) algorithm. Because of its high tracking accuracy, the method is widely used in the energy harvesting of PV systems. laboratory prototypes of the proposed SPO that have an input voltage range of 20 to 40 V and a maximum PV output power of 400 V/300 W are applied. Simulation results are carried out using MATLAB/Simulink model design.

Keywords: High step-up voltage gain, maximum power point tracking (MPPT), solar power optimizer (SPO)

1. Introduction

A power optimizer is a DC to DC converter technology developed to maximize the energy harvest from solar photovoltaic or wind turbine systems. They do this by individually tuning the performance of the panel or wind turbine through maximum power point tracking, and optionally tuning the output to match the performance of the string inverter. Power optimizers are especially useful when the performance of the power generating components in a distributed system will vary widely, differences in equipment, shading of light or wind, or being installed facing different directions or widely separated locations. Power optimizers for solar applications, can be similar to micro inverters, in that both systems attempt to isolate individual panels in order to improve overall system performance. A microinverter essentially combines a power optimizer with a small inverter in a single case that is used on every panel, while the power optimizer leaves the inverter in a separate box and uses only one inverter for the entire array. The claimed advantage to this "hybrid" approach is lower overall system costs, avoiding the distribution of electronics [2]. The proposed converter has the following features: 1) its voltage conversion ratio is efficiently increased by using the switched capacitor and coupled inductor techniques; 2) the leakage inductance energy of the coupled inductor can be recycled to increase efficiency, and the voltage spike on the active switch is restrained; 3) the floating active switch isolates the PV panel's energy during non operating conditions, thereby preventing any potential electric hazard to humans or facilities. The MPPT control algorithm exhibits high-tracking efficiency; hence, it is widely used in the energy harvesting of PV systems.

A conventional PV generation system is either a single- or a multi string PV array that is connected to one or several central PV inverters. Numerous series-connected PV modules are connected in the PV array to achieve the DC link voltage that is high enough to be connected to electricity through the DCAC inverter. However, the power reduction that is caused by the shadow effect is an inevitable problem in a centralized PV system. In the traditional grid-connected PV inverters, either a line frequency or a high-frequency transformer is utilized to provide a galvanic isolation between the grid and the PV panels. For a typical PV array, the output voltage is relatively low, and a high voltage gain is obligatory to realize the grid-connected function. A solar power optimizer (SPO) was developed as an alternative to maximize energy harvest from each individual PV module. Fig. 1 shows a single PV panel's energy, which passes through an SPO to a dc microgrid system. A 400 V dc-microgrid system was proposed as an energy-efficient distribution option for data center systems and telecommunication facilities.
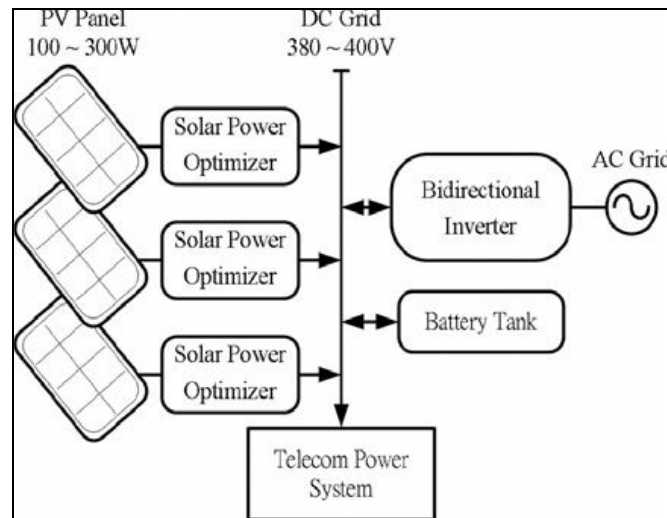
Figure 1: Configuration of multiple parallel SPO for a dcmicrogrid system

An SPO is used as a dc–dc converter with maximum power point tracking (MPPT), which increases PV panel voltage to optimum voltage levels for a dc microgrid connection. The SPO attempts to improve the use of distributed renewable resources and lower system cost. It may also potentially improve the efficiency of PV systems, has an anti shadow effect, and can monitor the status of PV modules. Moreover, the dc-grid voltage is regulated by bidirectional inverter and battery tank. In case of low-loading condition, the redundant energy will store into battery or through bidirectional inverter to ac grid.

2. Proposed System with its Principle of Operation
The proposed SPO is shown in Fig. 2; its configuration is based on a high step-up dc–dc converter with an MPPT control circuit.
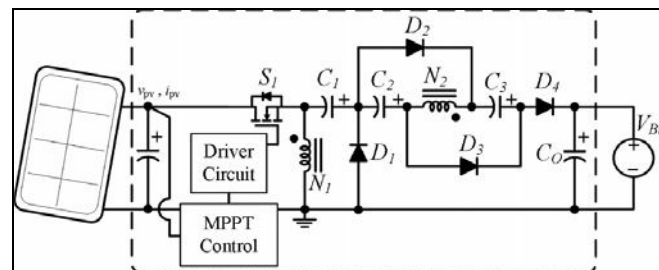

Figure 2: Configuration of the proposed SPO

The converter includes a floating active switch S and a coupled inductor $T1$ with primary winding $N1$, which is similar to the input inductor of a conventional boost converter capacitor $C1$, and diode $D1$ recycle leakage inductance energy from $N1$. Secondary winding $N2$ is connected to another pair of capacitors, $C2$ and $C3$, and to diodes $D2$ and $D3$. Rectifier diode $D4$ connects to output capacitor Co and load R. The duty ratio is modulated by the MPPT algorithm, which uses the incremental conductance method that is employed in the proposed SPO. It detects PV module voltage Vpv and current Ipv to determine the increase and decrease in the duty cycle of the dc converter. Therefore, the MPP can be obtained by comparing instantaneous conductance I/V and incremental conductance dI/dV. The proposed converter has the following features: 1) its voltage conversion ratio is efficiently increased by using the switched capacitor and coupled inductor techniques; 2) the leakage inductance energy of the coupled inductor can be recycled to increase efficiency, and the voltage spike on the active switch is restrained; 3) the floating active switch isolates the PV panel's energy during non operating conditions, thereby preventing any potential electric hazard to humans or facilities. The MPPT control algorithm exhibits high-tracking efficiency; hence, it is widely used in the energy harvesting of PV systems. The operating principles for continuous conduction mode (CCM) and discontinuous conduction mode (DCM) are presented in detail. Fig. 3 illustrates a typical waveform of several major components in CCM operation during one switching period. To simplify the circuit analysis of the proposed converter, the following assumptions are made:
1) All components are ideal, except for the leakage inductance of coupled inductor $T1$, which is taken into account. On-state resistance RDS (ON) and all the parasitic capacitances of main switch S are disregarded, as are the forward voltage drops of diodes $D1$ to $D4$;
2) Capacitors $C1$ to $C3$ and Co are sufficiently large that the Voltages across them are considered constant;
3)The equivalent series resistance (ESR) of capacitors $C1$ to $C3$ and Co, as well as the parasitic resistance of coupled inductor $T1$, is neglected;
4) Turns ratio n of coupled inductor $T1$ windings is equal to $N2$ /$N1$.

2.1. CCM Operation
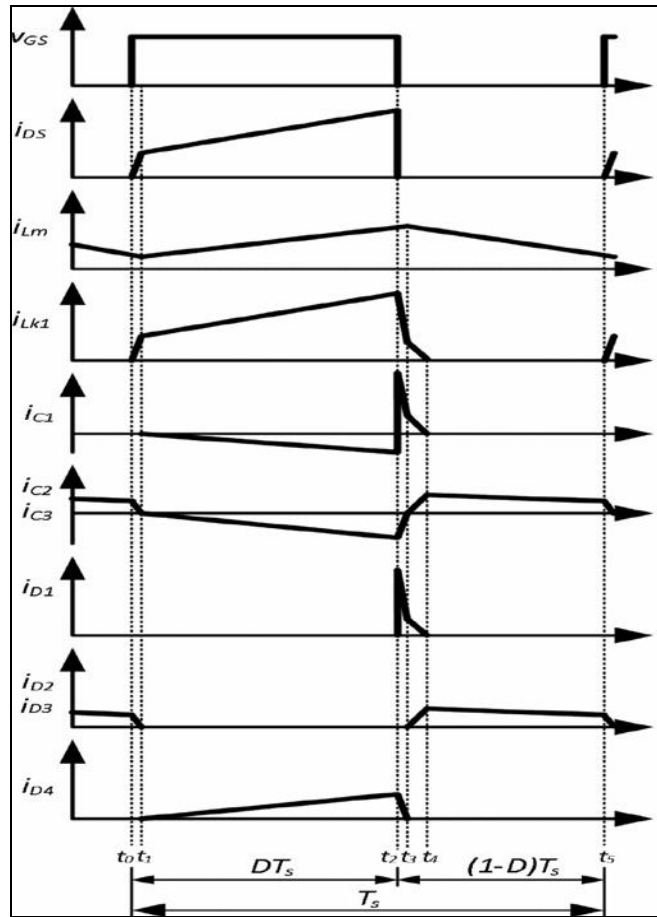The CCM operating modes are described as follows

Figure 3: Typical waveforms of the proposed converter in CCM operation

- Mode I [t0, t1]: During this interval, switch S and diodes D2 and D3 are conducted; diodes D1 and D4 are turned OFF. The current flow path is shown in Fig. 4(a). Magnetizing inductor Lm continues to release energy to capacitors C2 and C3 through secondary windingN2 of coupled inductor T1. Leakage inductance Lk 1 denotes the stored energy from source energy Vin. The energy that is stored in capacitor Co is constantly discharged to load R. This mode ends when increasing iLk1 is equal to decreasing *iLm* at $t = t1$

$vLm = Vin$ ……………. (1)

$\Delta iLm = Vin/Lm\ (t1 - t0)$. (2)
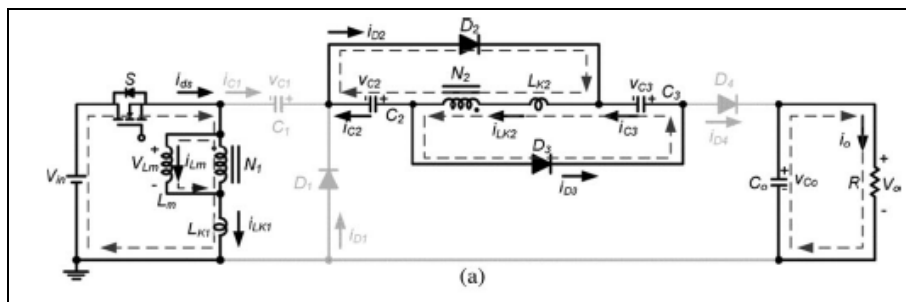
Figure 4 (a): Current flow path in five operatingmodes during one switching period in CCM operation Mode I

- Mode II [t1, t2]: During this interval, switch S and diode D4 are conducted. Source energy Vin is serially connected to C1, C2, and C3, and secondary winding N2 ; Lk2 discharges the energy that is stored in charge output capacitor Co and loads R. Meanwhile, magnetizing inductor Lm also receives energy from Vin . The current flow path is shown in Fig.(b). This mode ends when switch S is turned OFF at t = t2.

$$n = \frac{N_2}{N_1}$$

$$\Delta i_{Lm} = \frac{V_o - V_{in} - V_{c1} - V_{c2} - V_{c3}}{n \cdot L_m} \cdot (t_2 - t_1).$$
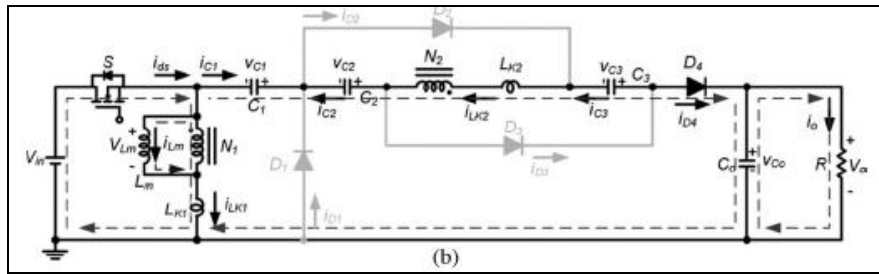

Figure 4 (b): Current flow path in five operatingmodes during one switching period in CCM operationMode II

• Mode III [t2, t3]: During this transition interval, switch S and diodes D2 and D3 are turned OFF, and diodes D1 and D4 are conducted. The current flow path is shown in Fig.(c). The energy stored in leakage inductance Lk 1 instantly flows through the diode D1 to charge capacitor C1 . The energy is released to magnetizing inductor Lm through coupled inductor T1, which is serially connected to C1, C2, and C3, and secondary winding N2; Lk2 discharges the energy that is stored in charge output capacitor Co and loads R. This mode ends when decreasing iLk1 is equal to increasing iLm at t =t3

$$v_{Lm} = -V_{c1}$$

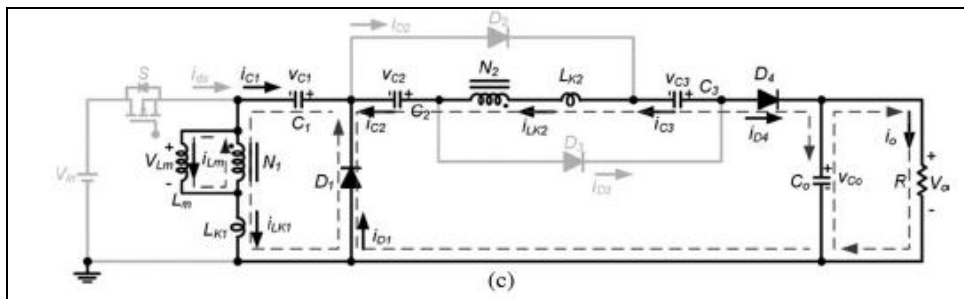$$\Delta i_{Lm} = \frac{-V_{c1}}{L_m} \cdot (t_3 - t_2).$$

Figure 4 (c): Current flow path in five operatingmodes during one switching period in CCM operationMode III

• Mode IV [t3, t4]: During this interval, switch S and diode D4 are turned OFF, and diodes D1,D2 , and D3 are conducted. The current flow path is shown in Fig.(d). Leakage inductance Lk 1 continues to release energy to charge capacitor C1 through diode D1. Magnetizing inductor Lm through coupled inductor T1 transfers energy to capacitors C2 and C3. The energy that is stored in capacitor CO is constantly discharged to load R. This mode ends when decreasing iLk1 is zero at t = t4.
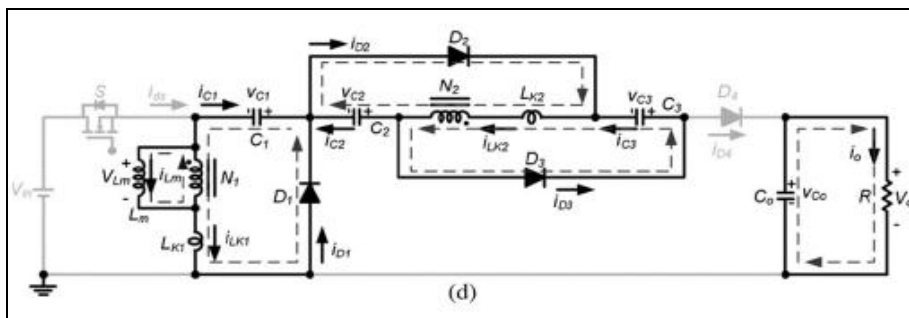

Figure 4 (d): Current flow path in five operatingmodes during one switching period in CCM operationMode IV

- Mode V [t4, t5]: During this interval, diodes D2 and D3 are conducted. The current flow path is shown in Fig.(e). Magnetizing inductor Lm constantly transfers energy to secondary winding N2 and charges capacitors C2 and C3. The energy that is stored in capacitor CO is constantly discharged to load R. This mode ends when switch S is turned ON at the beginning of the next switching period

$$v_{Lm} = \frac{-V_{c2}}{n} = \frac{-V_{c3}}{n}$$

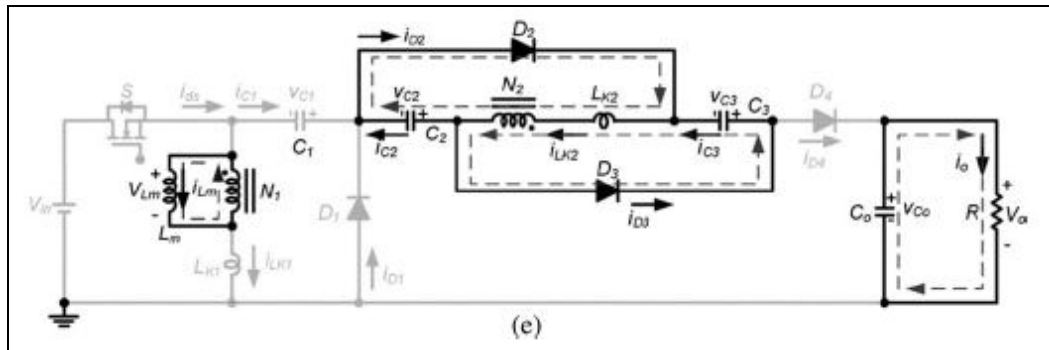$$\Delta i_{Lm} = \frac{-V_{c2}}{n \cdot L_m} \cdot (t_5 - t_4) = \frac{-V_{c3}}{n \cdot L_m} \cdot (t_5 - t_4).$$

Figure 4 (e): Current flow path in five operatingmodes during one switching period in CCM operationMode V

2.2. DCM Operation

- Mode I [t0, t1]: During this interval, switch S and D4 are conducted, and diodes D1, D2 , and D3 are turned OFF. The current flow path is shown in Fig. 6(a).Magnetizing inductor Lm with leakage inductance Lk 1 stores energy from source energy Vin. Meanwhile, source energy Vin is also serially connected to capacitors C1, C2 , and C3 , and secondary winding N2 to charge capacitor Co and load R. This mode ends when switch S is turned OFF at t = t1.

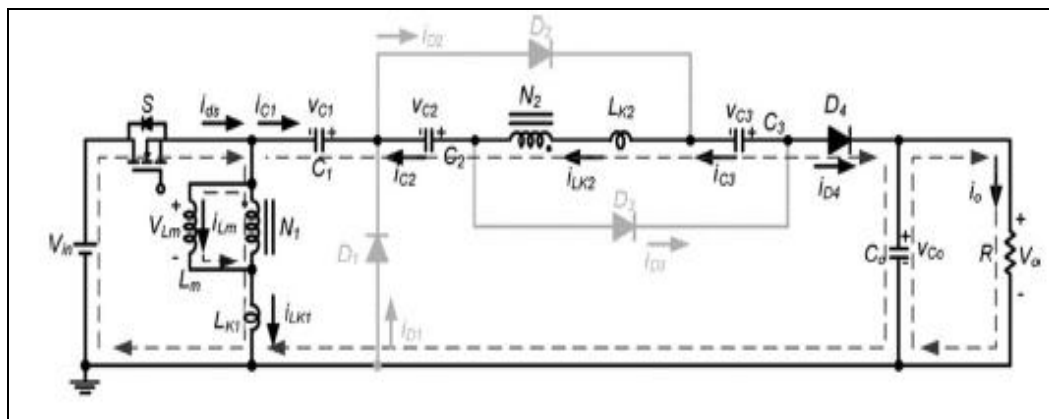$$v_{Lm} = V_{in} = \frac{V_o - V_{in} - V_{c1} - V_{c2} - V_{c3}}{n}$$

Figure 5 (a): Current flow path in five operatingmodes during one switching period in DCM operation Mode I

- Mode II [t1, t2]: During this transition interval, switch S and diodes D2 and D3 are turned OFF, and diodes D1 and D4 are conducted. The current flow path is shown in Fig. 6(b). The energy stored in leakage inductance Lk 1 instantly flows through the diodeD1 to charge capacitor C1 ; this energy is also released to magnetizing inductor Lm through the coupled inductor T1 series that is connected to C1, C2 , and C3 , secondary winding N2 , and Lk2 to charge output capacitor Co and load R. This mode ends when decreasing iD4 is zero at t = t2.
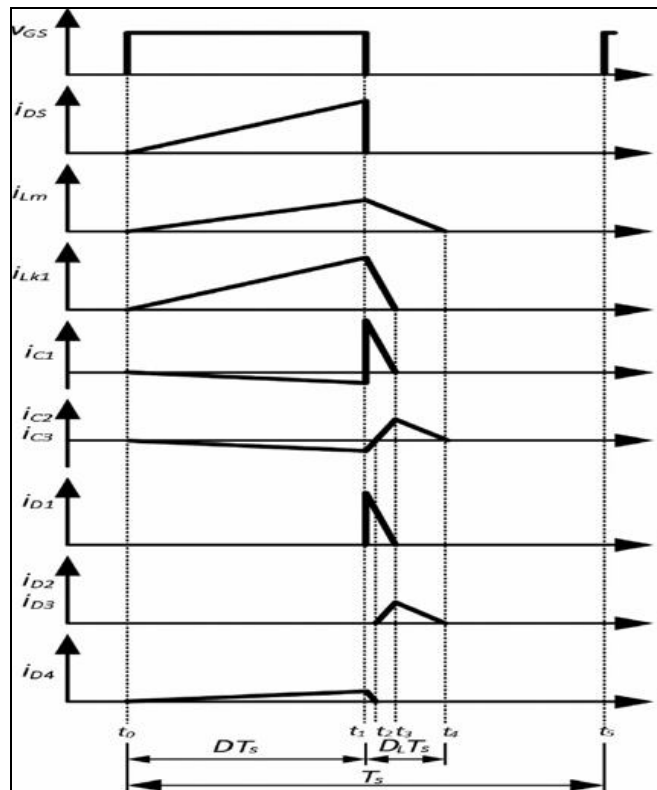
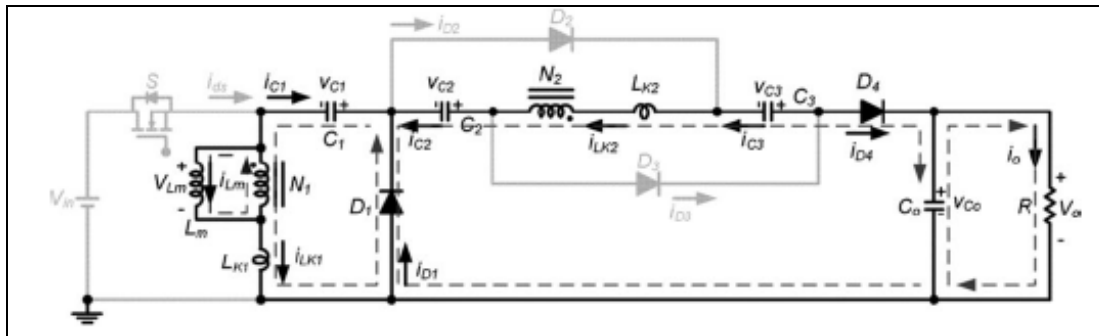*Figure 6: Typical waveforms of the proposed converter during DCM operation*

Figure 5 (b): Current flow path in five operating modes during one switching period in DCM operationMode II

- Mode III [t2 , t3]: During this transition interval, switch S and diode D4 are turned OFF, and diodes D1,D2 , and D3 are conducted. The current flow path is shown in Fig. 6(c). Leakage inductance Lk 1 continues to release energy to charge capacitor C1 through diode D1. Magnetizing inductor Lm transfers energy to capacitors C2 and C3 through coupled inductor T1. The energy stored in capacitor Co is constantly discharged to load R. This mode ends when decreasing iLk1 is zero at t = t3.

$$v_{Lm} = -V_{c1} = \frac{-V_{c2}}{n} = \frac{-V_{c3}}{n}$$

$$\Delta i_{Lm} = \frac{-V_{c1}}{n \cdot L_m} \cdot (t_3 - t_2) = \frac{-V_{c2}}{n \cdot L_m} \cdot (t_3 - t_2)$$
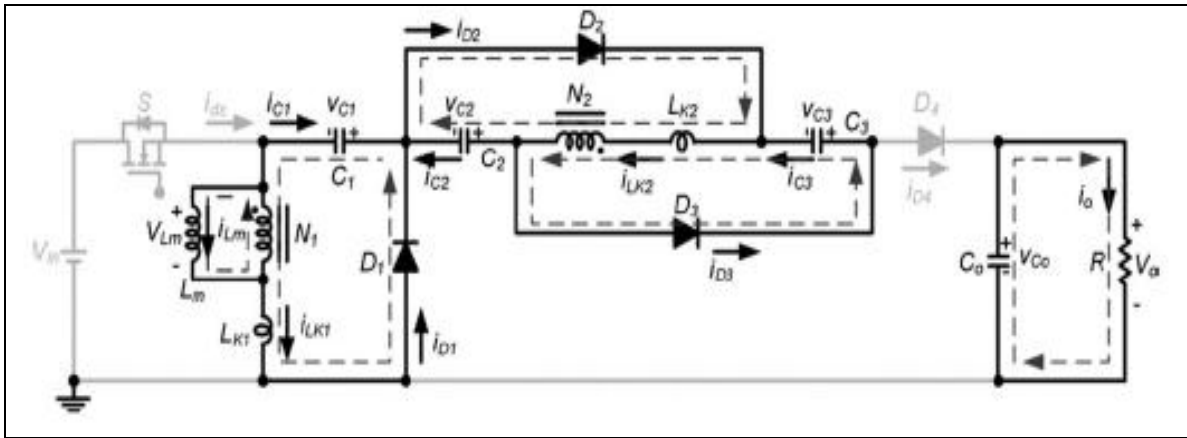
$$= \frac{-V_{c3}}{n \cdot L_m} \cdot (t_3 - t_2).$$

Figure 5 (c): Current flow path in five operatingmodes during one switching period in DCM operationMode III Mode IV [t3, t4]:

During this interval, switch S, diodes D1 and D4 are turned OFF, and diodes D2 and D3 are conducted. The current flow path is shown in Fig. 6(d).Magnetizing inductor Lm constantly transfers energy to secondary winding N2 and charges capacitors C2 and C3 . The energy that is stored in capacitor Co is constantly discharged to load R. This mode ends when decreasing iLm is zero at t = t4.
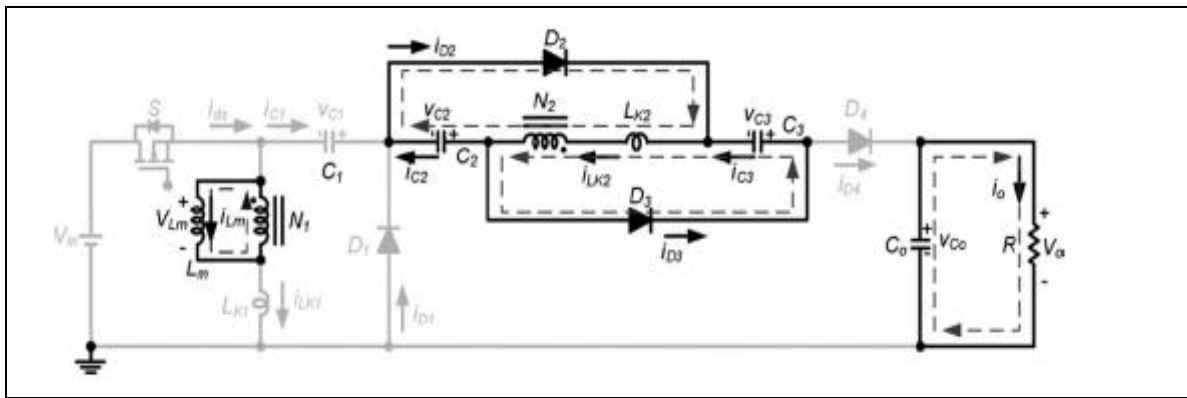

Figure 5 (d): Current flow path in five operating modes during one switching period in DCM operation Mode IV Mode V [t4, t5]:

During this interval, the switch and all the diodes are turned OFF. The current flow path is shown in Fig. 6(e). The energy that is stored in capacitor CO is constantly discharged to load R. This mode ends when switch S is turned ON at the beginning of the next switching period.
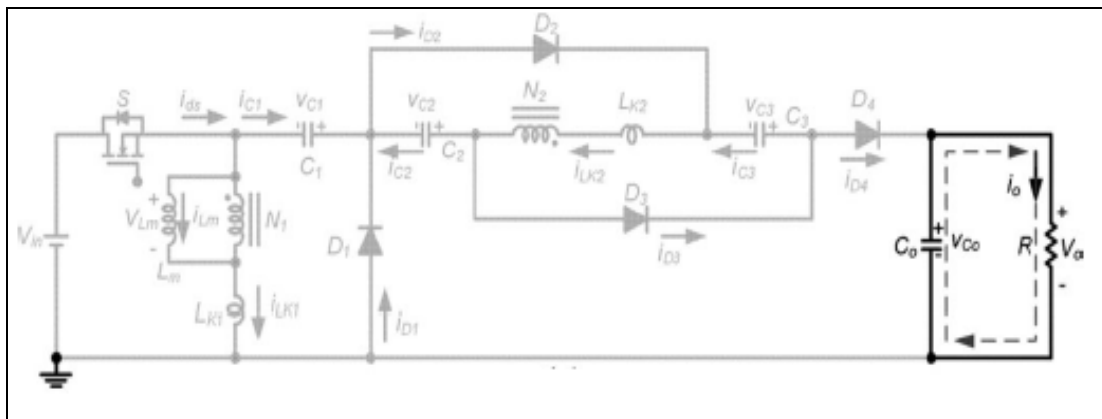

Figure 5 (e): Current flow path in five operatingmodes during one switching period in DCM operationMode V

3. Simulation Results
In the traditional grid-connected PV inverters, either a line frequency or a high-frequency transformer is utilized to provide a galvanic isolation between the grid and the PV panels. For a typical PV array, the output voltage is relatively
low, and a high voltage gain is obligatory to realize the grid-connected function.
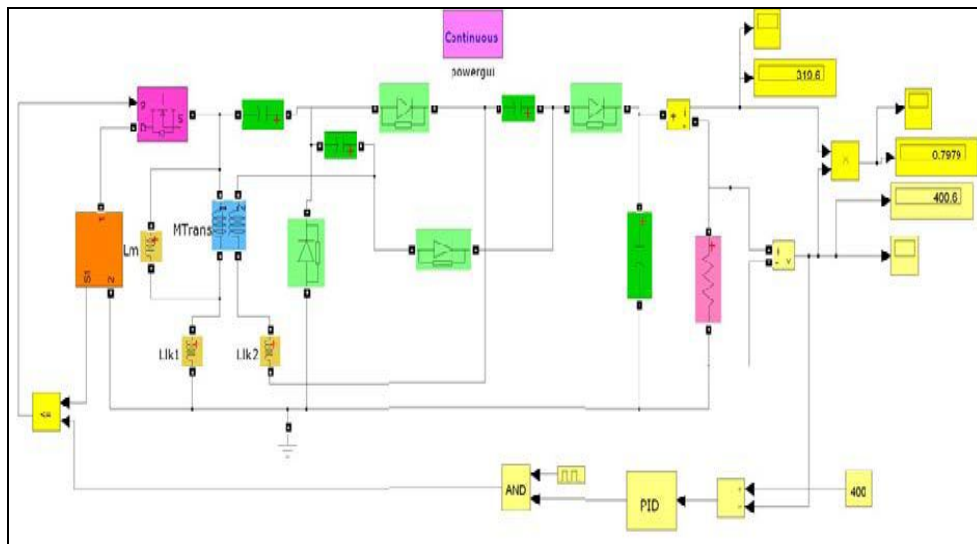
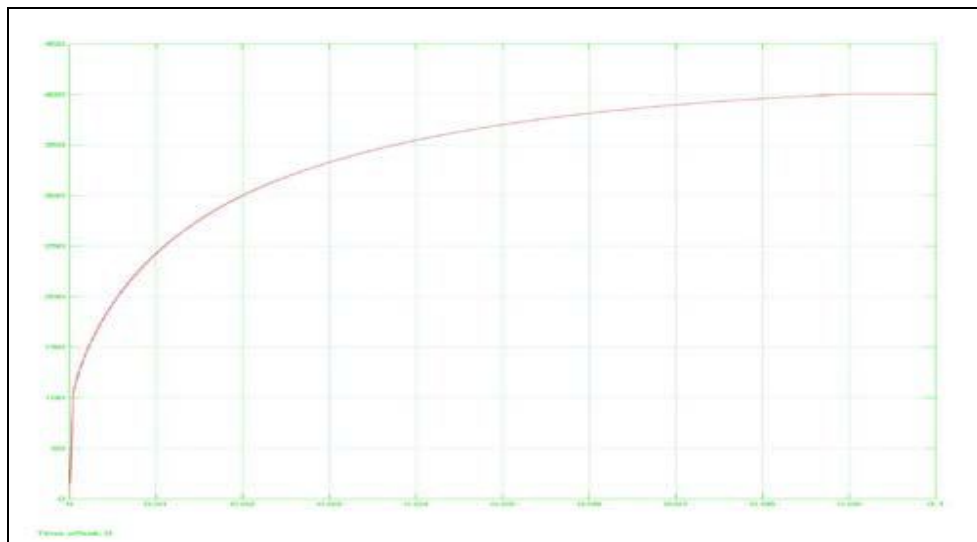*Figure 7: Closed loop circuit of solar power optimizer*
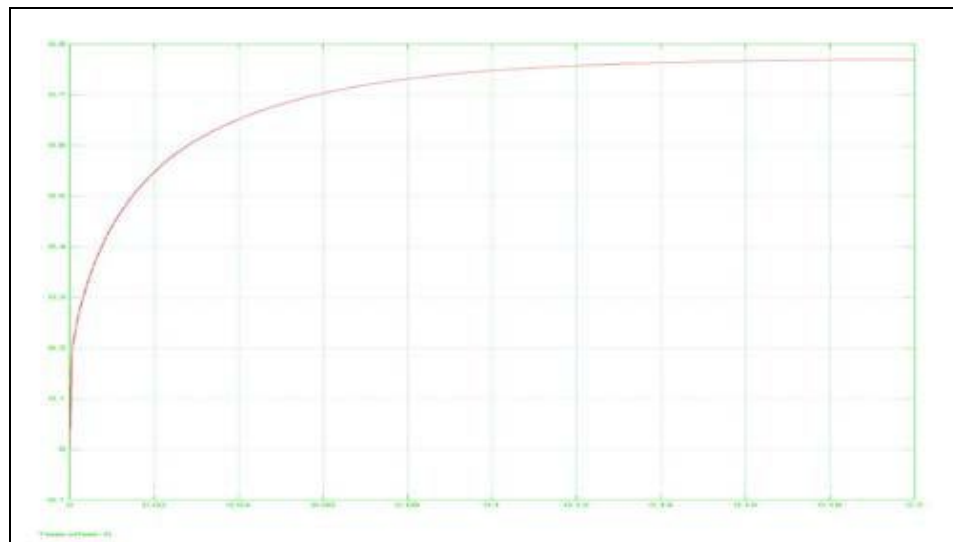

Figure 8: Output voltage waveform

Figure 9: Output current waveform

Figure 10: Output power waveform

3. Applications
1. High voltage application.
2. Tele communication.
3. Grid tie inverter & stand alone inverter

4. Conclusion
The high step-up SPO uses the coupled inductor with an appropriate turn's ratio design and switched-capacitor technology to achieve a high-voltage gain higher than the input voltage. Because the leakage inductance energy of a coupled inductor is recycled and the voltage stress across the active switch S is constrained, the low RDS (ON) of active switch can be selected to improve maximum efficiency. A 300 W SPO with a high step-up voltage gain and MPPT functions are implemented and verified using MATLAB Simulink model design.

5. Future Scope
The system can be extended for more voltage range. Increase in more voltage range will increases the voltage gain and efficiency of the converter system. The output DC voltage can be inverted and we can use the AC loads also

6. References
1. W. Yu, J.-S. Lai, H. Qian, and C. Hutchens, "High-efficiency MOSFET inverter with H6-type configuration for photovoltaic non isolated ac-module applications," IEEE Trans. Power Electron., vol. 26, no. 4, pp. 1253–1260, Apr. 2011.
2. L. Gao, R. A. Dougal, S. Liu, and A. P. Iotova, "Parallel-connected solar PV system to address partial and rapidly fluctuating shadow conditions," IEEE Trans. Ind. Electron., vol. 56, no. 5, pp. 1548–1556, May 2009.
3. R. Gules, J. De Pellegrin Pacheco, H. L. Hey, and J. Imhoff, "A maximum power point tracking system with parallel connection for PV stand-alone applications," IEEE Trans. Ind. Electron., vol. 55, no. 7, pp. 2674–2683, Jul. 2008.
4. B. Liu, S. Duan, and T. Cai, "Photovoltaic dc-building-module-based BIPV system: Concept and design considerations," IEEE Trans. Power Electron., vol. 26, no. 5, pp. 1418–1429, May 2011.
5. W. Xiao, N. Ozog, and W. G. Dunford, "Topology study of photovoltaic interface for maximum power point tracking," IEEE Trans. Ind. Electron., vol. 54, no. 3, pp. 1696–1704, Jun. 2007.
6. L. Zhang, K. Sun,Y. Xing, L. Feng, andH.Ge, "A modular grid-connected photovoltaic generation system based on DC bus," IEEE Trans. Power Electron., vol. 26, no. 2, pp. 523–531, Feb. 2011.
7. S.M. Chen, T. J. Liang, L. S. Yang, and J. F. Chen, "A boost converter with capacitor multiplier and coupled inductor for AC module applications," IEEE Trans. Ind. Electron., Early Access Articles, vol. PP, no. 99, p. 1.
8. A. C. Nanakos, E. C. Tatakis, and N. P. Papanikolaou, "A weighted efficiency- oriented design methodology of flyback inverter for AC photovoltaic modules," IEEE Trans. Power Electron., vol. 27, no. 7, pp. 3221–3233, Jul. 2012.
9. S. Zengin, F. Deveci, and M. Boztepe, "Decoupling capacitor selection in DCM flyback PV micro-inverters considering harmonic distortion," IEEE Trans. Power Electron., Early Access Articles, vol. pp., no. 99, p. 1.
10. B. Axelrod, Y. Berkovich, and A. Ioinovici, "Switched-capacitor/switched-inductor structures for getting transformerless hybrid DC-DC PWM converters," IEEE Trans. Circuits Syst. I, Reg. Papers, vol. 55,no. 2, pp. 687–696, Mar. 2008.
11. O. Abutbul, A. Gherlitz, Y. Berkovich, and A. Ioinovici, "Step-up switching-mode converter with high voltage gain using a switched- capacitor .circuit," IEEE Trans. Syst. I, Fundam. Theory Appl., vol. 50, no. 8, pp. 1098–1102, Aug. 2003